Solar Physics
DOI: 10.1007/**********

Dynamics of Explosive Events by Interface Region Imaging Spectrograph

E. Tavabi [1] · S. Zeighami [2*] · M. Heydari [1]

Received: ******* / Accepted: **********

Abstract In this research, we investigate Explosive Events (EEs) in the off-limb solar atmosphere, with simultaneous observations from the Si IV, Mg II k, and slit-jaw images (SJI) based on the Interface Region Imaging Spectrograph (IRIS), on 2014 August 17, and February 19. IRIS data can be investigated to observe the motion of matter, fluctuations, energy absorption, and heat transition of the solar atmosphere. Mechanisms responsible for solar large-scale structures, such as flares and coronal mass ejections might be originated from these small-scale energetic events. Therefore, study of these events can be helpful for understanding mechanisms in mass and energy transporting from chromosphere toward transition region and corona. We obtain intensity profiles from spectra in two altitudes i.e., solar limb and 5 arcsec distance from solar limb, and then analyze the EEs fluctuations at two altitudes along the slit. We observed that some line profiles of spectra show enhancements in blue and red wings indicating outward and downward flows, and some profiles represent opposite EEs on their both wings. The Amplitude of the Doppler velocity in two data for the two altitudes was approximated to be about 50 km/s. We calculated the phase velocity of the oscillations using a technique based on cross-correlation. The phase velocity is obtained as about 220 km/s. According to the periodic red and blue enhancements in EEs, we suggested that the fluctuations in the EEs with one side enhancement indicate the swaying motions of spicules over their axes, and those EEs which observed on both wings indicate the rotational motions of spicules. The swaying and rotating motions are responsible to the kink and twisted waves respectively.

✉ E. Tavabi
e_tavabi@pnu.ac.ir
✉ S. Zeighami
zeighami@iaut.ac.ir
M. Heydari
mehriheidari95@yahoo.com
[1] Physics Department, Payame Noor University (PNU), 19395-3697-Tehran, I. R. of Iran
[2] Department of Physics, Tabriz Branch, Islamic Azad University, Tabriz, Iran

Keywords Transition Region · Explosive Events · Coronal Heating · Phase Velocity

1. Introduction

EEs are dynamic events that first were observed from the solar transition region (TR) with the high-Resolution Telescope and Spectrograph (HRTS) (Brueckner *et al.* 1993). EEs could generate non-Gaussian profiles with strong enhancement. EEs have a spatial extension of 1-2 arcsec, and typical lifetime of roughly 60 s (Chen et al. 2019). It was first believed that such spectra are emitted from turbulent events (Brueckner *et al.* 1983), and for this reason, they are called explosive events (Dere *et al.* 1984). Thereafter the term of transition region explosive events (TREEs) are used (Dere *et al.* 1984). Some EEs could also produce enhancements in spectra of CI, CII, OI, and MgII (Dere 1992, Zhang *et al.* 2010, and Tavabi and Koutchmy 2019). EEs are repeatedly appeared in observations (Chae *et al.* 1998, Ning *et al.* 2004, and Doyle *et al.* 2006), which might be caused by magnetic reconnection in the upper chromosphere modulated by p-mode oscillations. Non-Gaussian line profiles of EEs could be generated by spinning, unwinding, or twisting motions (Curdt *et al.* 2012, De Pontieu *et al.* 2014a). In De Pontieu *et al.* (2014a) authors found that twisting motions of small-scale TR loops and jets can result in EE-type line profiles of EEs. In Chen *et al.* (2019), using simultaneous imaging and spectroscopic observations from IRIS, the link between EEs and network jets was investigated. Their analysis suggests that some EEs are related to the birth or propagation of network jets, and the others are not connected to network jets. The energy source required to heat the solar corona plasma to a temperature of more than one million Kelvin in the solar dynamic photosphere is a subject of debate in solar physics. The transmission of energy through waves and oscillations can play an important role in understanding the solar dynamics structures and the cause of the sudden rise in temperature of the solar atmosphere to several million Kelvin from the transition region to the solar corona (De Pontieu et al. 2007c). One of the energy transfer mechanisms is the propagation of magneto-hydrodynamic waves (Roberts *et al.* 2004). These waves in photospheric magnetic tubes can be generated by granular shock motions and then propagate along the chromosphere and penetrate the corona to transfer energy as heat. Therefore, observations of oscillating motions in the solar atmosphere are a key test for the theory of coronal heating. The chromosphere layer of the solar atmosphere is composed of structures called spicules. The cut-off period in the chromosphere is 3 minutes (De Pontieu *et al.* 2004). This means that only waves with a period of less than 3 minutes can penetrate the higher layers. Spicules have diameters from about 120 km to 700 km, and their maximum lengths vary from a few hundred kilometers to 10,000 km with most below 5,000 km (De Pontieu *et al.* 2007c, 2012). Chromospheric

spicules at the limb in coronal holes are intimately linked to the formation of features at TR and coronal temperatures (De Pontieu *et al*. 2007c).

Jets are narrow gas eruptions about 150 to 500 kilometers in diameter launched from the top of an almost homogeneous layer that stretches for about 3,000 kilometers. Needle-shaped spicules accumulate in areas of the solar supergranular network. Spicules are plasma explosions that occur almost every 5 minute. Spicules are present even in the quiet Sun. Spicules are ubiquitous, high-velocity jets found in the spectral lines of the dark chromospheric edge. Combining recent spectroscopic images of projectiles with solar observations has made it possible to study spicules motion and their disappearance (Tavabi *et al.* 2015a, and (Tavabi *et al.* 2015b). Recent studies have shown that spicules appear in several transitional and chromospheric lines of the solar atmosphere, and it is speculated that the spicules, after disappearing, appear as jets in the transition region in hot regions (De Pontieu et al. 2007c and 2011, Pereria *et al*. 2014). The purpose of studying the spicules and their properties in different parts of the Sun is to obtain information about chromosphere layer that is a dynamic region and is of special importance in solar physics. The reason for appearing the spicules in the corona in the form of moving spicules is that the density of the chromosphere does not correspond to the density of the corona material. Spicules play an important role in the mass equilibrium of the solar corona. The brightness of the spicules changes with temperature and altitude, and spectroscopic studies provide valuable information about the spicules through changes in the profile of the spectral lines. Doppler shift in these lines determine the velocity in the line of sight (Sekse et al. 2012 and 2013, Bose et al. 2019 and 2021, Kuridze *et al*. 2015) and its changes with time and altitude from the surface of the Sun (Tavabi *et al.* 2015a). By widening the spectral lines, it is possible to measure non-thermal rotational velocities that lead to the indirect observation of torsional Alfven waves. Many of them have a diameter of 400 to 1500 km. Spicules can heat the corona both by expelling hot plasma and by transferring energy by magneto-hydrodynamic waves (Rouppe van der Voort *et al.* 2009, Zeighami *et al.* 2016). So far, two types of spicules have been identified (De Pontieu et al. 2007c, Pereria et al. 2012). Type II spicules have a typical lifetime of 150-400 seconds with upward and downward motions on the parabolic paths with a maximum upward speed of 15-40 km/s, and the II type have only upward motions with a lifetime up to 50-150 seconds, and a speed of 30 -110 km/s (See figure 4 in Pereria *et al*. 2012). Rouppe van der Voort *et al.* (2009), studied statistical properties of the disk counterparts of type II spicules from observations of Rapid Blue-shifted Excursions (RBEs), and found that the appearance, lifetimes, longitudinal and transverse velocities and occurrence rate of these rapid blue excursions on the disk are very similar to those of the type II spicules at the limb. Pereria *et al*. 2012 investigated the type I spicules and found relations between their properties with a magnetoacoustic shock wave driver and with dynamic

fibrils as their disk counterpart. They also found that the properties of type II spicules are consistent with properties of Rapid Blueshifted Events (RBEs), conirming the hypothesis that RBEs are their disk counterparts. Type II spicules mainly present in both the quiet Sun and coronal holes, but in active regions the type I are predominant (Pereria *et al.* 2012). A recent study of observations from the Hinode and IRIS satellites showed that Type II spicules are heated up to the TR and coronal hole temperatures (Pereira *et al.* 2014, De Pontieu *et al.* 2011). The disk counterparts of type II spicules have been identified through the asymmetry of short-lived chromospheric spectral lines and are inferred as the rotation of blue or red shifts (Langangen *et al.* 2008, Rouppe van der Voort *et al.* (2009), Kuridze *et al.* (2015), and Bose *et al.* (2019). Image processing and spectral methods are used to analyze the motion of structures such as spicules and solar jets. In the image processing method, displacements and intensity changes in images are measured (Tavabi *et al.* 2015b). In the second method, periodic designs in Doppler shifts are examined by spectrometers (Tavabi *et al.* 2015a, Tavabi 2018, Tavabi and Koutchmy 2019, and Zeighami *et al.* 2020).

In this study, we investigate the solar off-limb EEs based on IRIS observations, and then analyze the line spectra, on 2014 August 17, and February 19. IRIS provides a tool for analyzing the thermal structure of the solar atmosphere in the UV wavelength with high spatial and temporal resolution (De Pontieu *et al.* 2014).

2. Observations

In this study we analyzed two level 2 datasets from the IRIS database. IRIS spacecraft contained a combination of telescope and spectrograph (De Pontieu *et al.* 2014). IRIS obtains observations of the solar transition region with high spatial and spectral resolution to investigate the physical processes of fine structures (Chen *et al.* 2019, Tavabi and Koutchmy. 2019, Zeighami *et al.* 2020, Bose *et al.* 2021a). The spectral dispersion in the far and near-ultraviolet are about 0.025 Å and 0.053 Å, respectively. The first data with OBSID 380011404, is a very large sit-and-stare observation of a limb filament target, taken on 2014 August 17 from 10:06:13 UT to 13:59:48 UT. The Slit-Jaw Images (SJIs) field of view is 175” x 167” with cadence 32 s in both 2796 Å and 1400 Å filters. The center of the slit is centered at X = 827” and Y = -465” in the heliocentric coordinate with a roll angle of -45 degrees. The cadence of the spectral observation is 16 s. The spatial pixel size is about 0.167” per pixel for both the spectral and sj images. The second data with OBSID 3800258253, is a large site- and -stare observation of a limb spicules target, taken on 2014 February 19, from 16:27:46 UT to 17:35:45 UT. The Slit-Jaw Images (SJIs) field of view is 119” x119”, with cadences 23s and 19 s in 1330 Å and 1400 Å filters, respectively. The center of the slit is centered at X = 6” and Y = -980” in the heliocentric coordinate with no roll angle. The cadence of this data is 9 s. The top panels of Figure 1 show the SJI images in 2796 Å and

1400 Å taken from the IRIS, on August 17, 2014, and bottom panels show the SJI images in 1330 Å and 1400 Å taken from the IRIS, on February 19, 2014. The vertical lines in the panels refer to the location of the slit. It is noted that the effect of solar rotation with long time about 3 hour data set can be neglected.

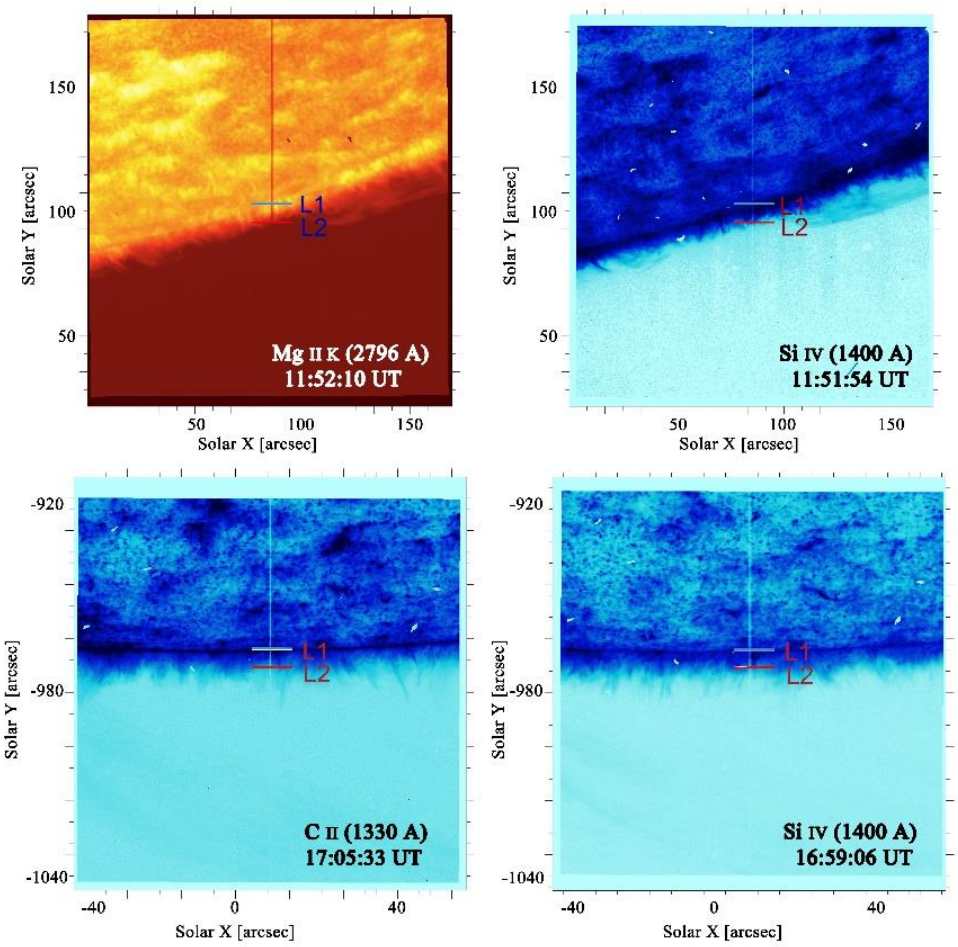

Figure 1 Top panels show the SJI images in 2796 Å and 1400 Å filters taken from the IRIS, recorded on August 17, 2014. The bottom panels show the SJI images in 1330 Å and 1400 Å taken from the IRIS, recorded on February 19, 2014. The vertical lines in the panels refer to the location of the spectrograph slit, and two short green lines refer to altitudes along which time slices are calculated.

3. Data Analysis

For analyzing spectral images, we first apply an unsharp mask method for all images, and then select a time interval in which can be seen Doppler shifts with significant fluctuations (red and blue shifts) with respect to the central wavelength. The ranges for the two data are about 106 minutes and 68 minutes, respectively. Blue and red shifting mean moving the structure of the event closer to the observer and far from the observer, respectively. We obtain intensity profiles from the spectral images along two altitudes, i.e., at the solar limb and Y=5 “far from the solar limb. In this way, time slices images of the profiles can be ready. Some profiles enhance at both the blue and red wings, show two peaks with comparable magnitude, and some profiles enhance only at the blue wing or red wing. Chen *et al.* (2019) obtained similar profiles. The left panels of figure 2 represent examples of Si IV 1403 Å and Mg II k 2796 Å spectra belonged on 2014 August 17, the two white lines refer to altitudes along which time slices are calculated, and right panels show temporal evolution of Si IV 1403 Å and Mg II k 2796 Å along two latitude which indicated by two white lines on the left panels. The left panels of figure 3 represent examples of Si IV and Mg II k spectra belonged on 2014 February 19, the two white lines named by L1 and L2, refer to altitudes along which time slices are calculated, and right panels show temporal evolution of Si IV 1403 Å and Mg II k 2796 Å along two latitude which indicated by two white lines on the left panels.

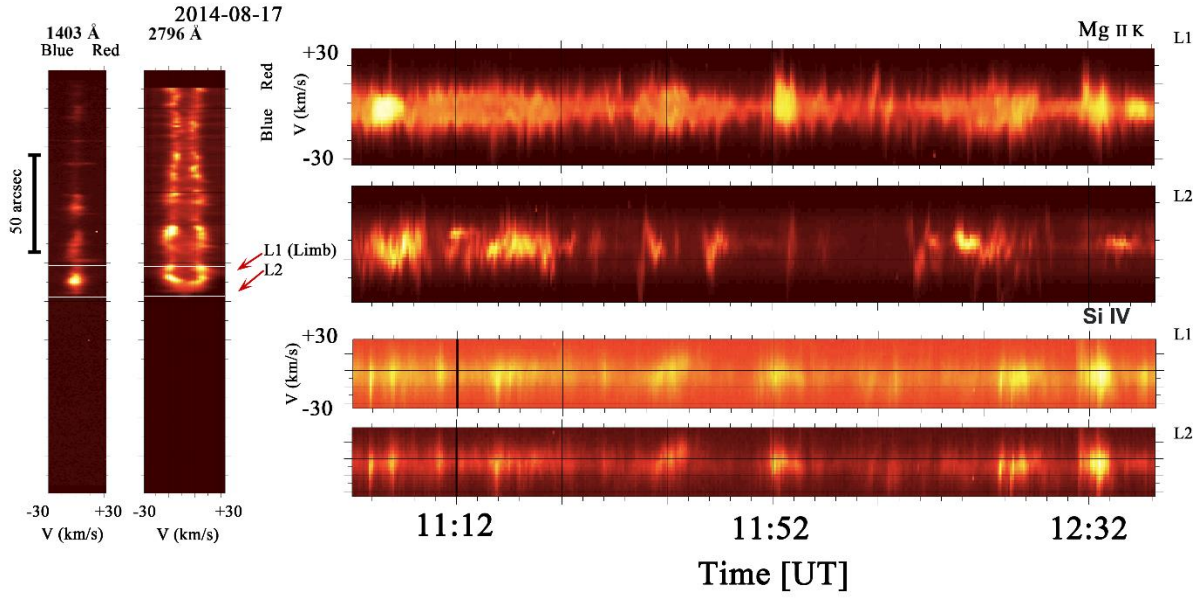

Figure 2 Left panels represent examples of Si IV 1403 Å and Mg II k 2796 Å spectra observed on 2014 August 17. The two white lines named by L1 and L2, refer to altitudes along which time slices are calculated. The right panels show temporal evolution of Si IV 1403 Å and Mg II k 2796 Å along two altitudes indicated by two white lines on the left panels.

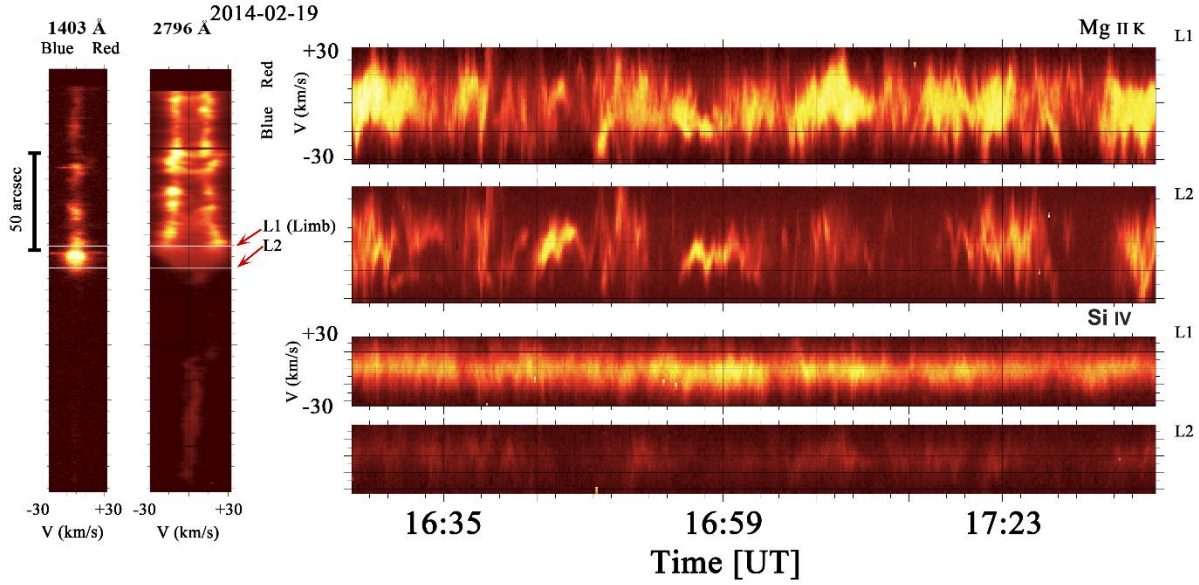

Figure 3 Left panels represent examples of Si IV 1403 Å and Mg II k 2796 Å spectra recorded on 2014 February 19. The two white lines refer to altitudes along which time slices are calculated. The right panels show the temporal evolution of Si IV 1403 Å and Mg II k 2796 Å along the two altitudes indicated by two white lines on the left panels. The horizontal lines on the right panels indicate the rest wavelength position Mg II k 2796 Å and Si IV 1403 Å spectra.

Figure 4 shows the examples of the EEs with non-Gaussian profiles in Si IV 1403 Å line. Panels a—c belong to the first data 2010817, and panels d—f belongs to the second data. It is seen blue, both blue and red, and red shift from left to right, respectively.

Tavabi et al. (2015) studied short-duration but complex jets related to a limb-event brightening (LEB) or limb EE directly above the South polar limb. At the Si IV emission temperature they observed a pair of rapidly moving separated parts looking like two split branches (emission lines exhibit Doppler shifts toward red and blue, as one would expect from a bidirectional jet (Innes et al. 1997) at TR temperatures, with a narrow 400 km space between them in the radial direction and another part nearby rapidly moving in the opposite direction. Bidirectional jets in such events are accelerated in opposite directions from the reconnection sites, the first approximation null-point reconnection geometry could imply the involvement of magnetic loops, separatrix surfaces, and spine for which outflow jets are expected to have a

multidirectional structure, which indeed has been observed in the form of simultaneous blue and red Doppler shifts in the limb EE. The bidirectional plasma jets ejected from a small reconnection site are interpreted to be the result of chromosphere or TR small loop–loop interactions that lead to reconnection in nearby sites. These observations are compatible with the following scenario: Similar to another observationally motivated scenario and three-dimensional models for Ellerman bombs, serpentine magnetic field lines form in the process of flux emergence, which produce magnetic dips in the photosphere. The corresponding opposite polarities at the bomb locations are clear.

Si IV line is optically thin, except for events such as flares, but the Mg II lines are optically thick lines with a strong central reversal in the line cores (See Figure 5). Leenaarts *et al.* (2013 a,b) studied the general formation mechanism of this line. Bose *et al.* (2019, 2021b) showed that the position of the maximum intensity named k2, is significantly affected by opacity effects in the solar chromosphere and the Doppler-shift of the line center which named k3. The k3 line minimum are used as an actual representative of the mass flow. For eleminating cosmic rays and finding doppler velocity we subtract the averaged over the whole of spatial and temporal profiles from each profile per pixel (Tavabi and Koutchmy 2019).

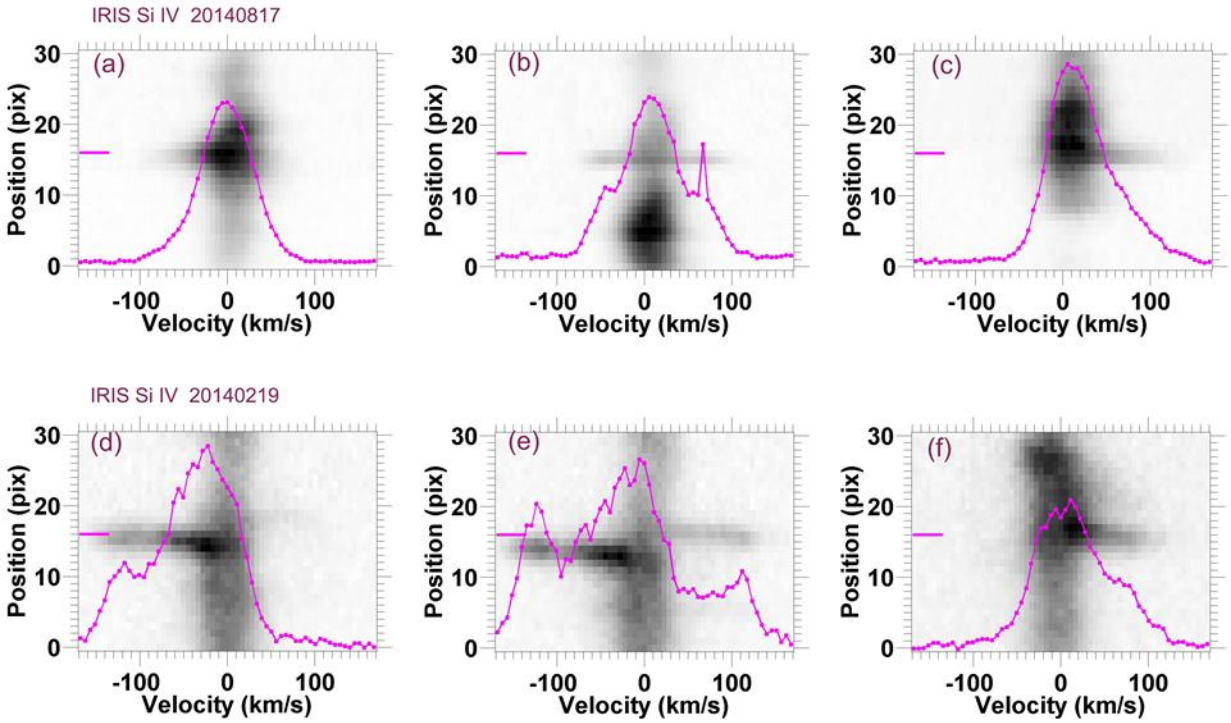

Figure 4 Examples of the EEs with non-Gaussian profiles in Si IV 1403 Å line. Panels a—c belong to the first data 2010817, and panels d—f belongs to the second data. It is seen blue, blue and red, and red shift from left to right, respectively.

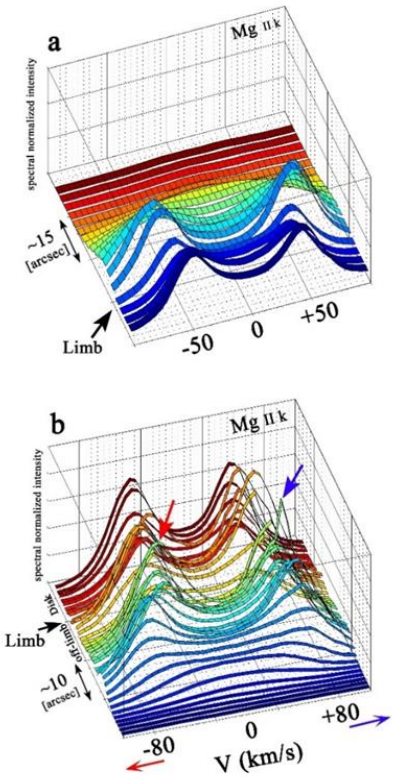

Figure 5 Top and bottom panels are the line profiles of Mg II k 2796 Å spectra plotted as a function of velocity recorded on 2014 August 17 and February 19, respectively.

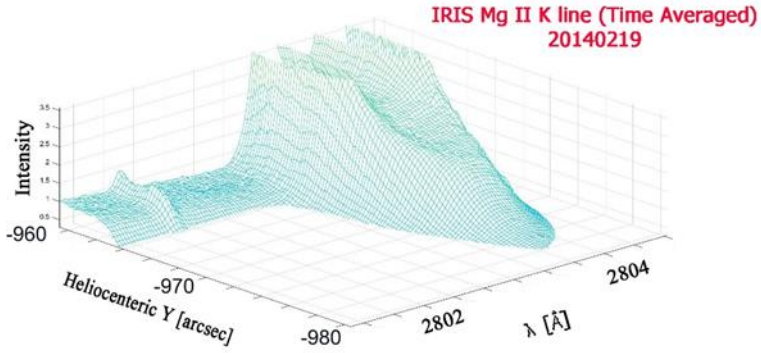

Figure 6 IRIS Mg II k 2796 Å line spectra (Time-averaged) which are plotted versus wavelength, and Y position (Heliocentric) recorded on February 19, 2014.

Peter et al. (2014) studied hot Explosions in the Cool Atmosphere of the Sun, and demonstrated C II and the Mg II lines show a structure similar to Si IV farther away from the self-absorption center. They found that it is reasonable to assume that the plasma ejected in the explosion covers temperatures from 6000 K to 100,000 K. This supports the conclusion that they observe a multi-thermal reconnection outflow. They In the bombs the Mg II lines show profiles that are very similar to Si IV. Therefore it might be that the outer parts (in the wing) of Mg II are a reflection of the reconnection outflow, indicating a strong flow with a magnitude similar to what is also seen in Si IV in the cooler plasma where Mg II originates. The maximum intensity of line spectrum is not the main true LOS velocity, however it shows the certainly true evidence of averaged Doppler velocities and more trustable. The principal tool for analyzing the LOS velocity structure of the upper atmosphere is spectroscopy at ultraviolet wavelengths, where IRIS provides high spatial, temporal, and spectral resolution. They showed an average spectrum for the limb above the quiet Sun region with the C II, Si IV, and Mg II lines. The line profiles generally conform to a single Gaussian, where they form under optically thin conditions. The lines of Mg II show self-absorption in the center due to large opacity. According to this suggestion and because all absorption lines are shifted they satisfied that the emission lines seen in the C II, Si IV and Mg II are primarily due to chromospheric (and TR) material directly above the EEs that is lifted in the flux-emergence process and cause the Doppler shifts.

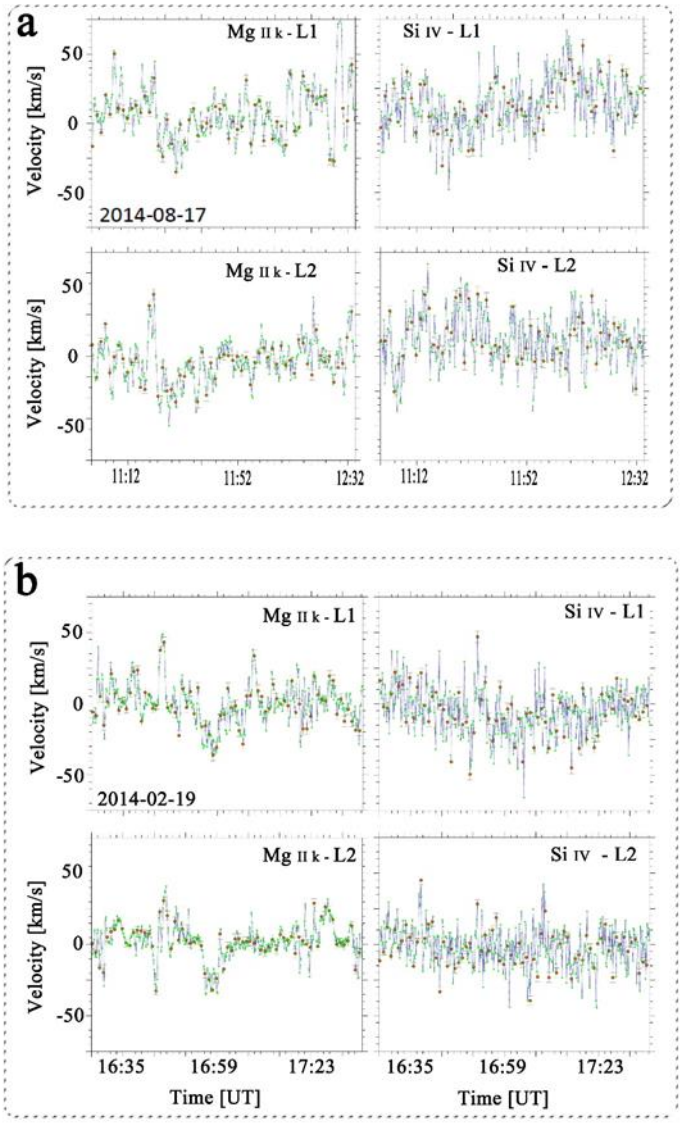

Figure 7 (a) and (b) Temporal evolution of Doppler velocity obtained from images taken in Si IV 1403 Å and Mg II k 2796 Å spectra on 2014 August 17 and February 19, respectively. The red circles indicate the Doppler velocity on the time slices of Figures 1 and 2.

After determining the doppler velosity at every time-slice in figures 2 and 3and For exact analysis of these EEs we plot separately the doppler velosity versus time.

Figure 5 from top to bottom shows the line profiles of Mg II k spectra plotted as a function of velocity recorded on 2014 August 17 and February 19, respectively. Figure 6 shows IRIS Mg II k 2796 Å line spectra (Time- averaged) which are plotted versus wavelength, and Y position (Heliocentric) recorded on

February 19, 2014. Figure 7 from top to bottom illustrate the temporal evolution of Mg II k 2796 Å and Si IV 1400 Å spectra for the two altitudes, which recorded on 2014 August 17 and February 19. The red circles indicate the position of doppler velocity on the time slices of Figures 1 and 2. As figure 7 shows, it can be seen that EEs have oscillatory behavior. For investigating correlation between limb and off limb intensity oscillations the two profiles are obtained. Figure 8 indicates the temporal evolution of spectra intensities on 2014 February 19 from Mg II 2796 Å line intensity for two signals with a height difference Y=5 arcsec. The blue and red colors refer to the first signal near the limb and the second signal at distance Y=5 arcsec respectively. Figure 9 indicate temporal evolution of Doppler velocity obtained on 2014 February 19 from Mg II k 2796 Å line intensity for two signals with height difference. The blue and red dashed lines refer to the first signal (near the limb) and the second signal (with distance of Y=5 arcsec), respectively. As figure 9 shows, there are correlation between two signals at certain times. We calculated the phase velocity of the two signals using a technique based on cross-correlation (Zeighami *et al.* 2020). In this method, time-lag between the two signals is calculated, and then by considering the distance between two altitudes (Y=5 arcsec or 4000 km), the phase velocity is calculated. The phase velocity is obtained about 220 km/s.

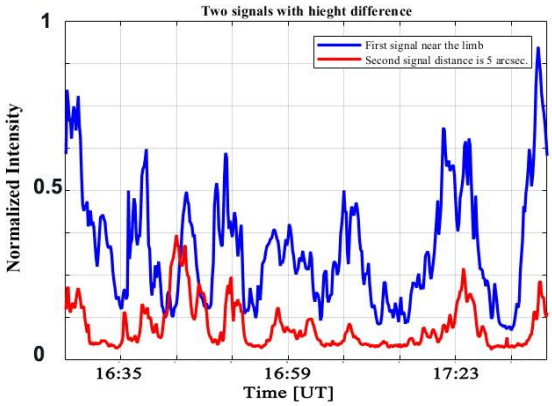

Figure 8 Normalized intensity of two signals with height difference taken on 2014 February 19, the first and second signals are shown by blue and red colors, respectively.

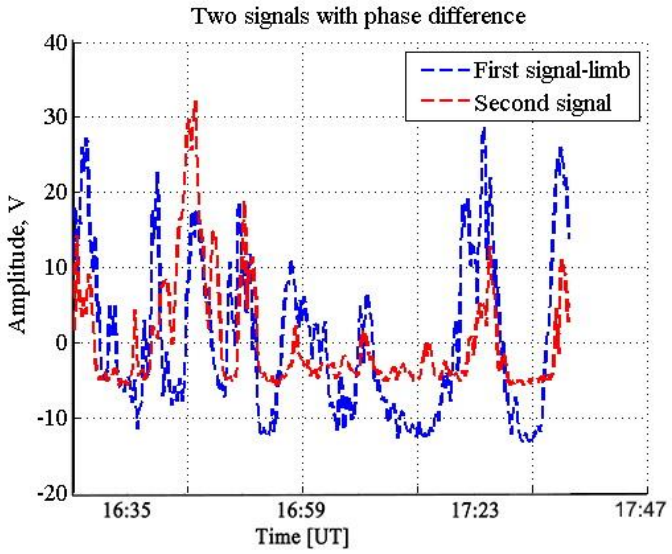

Figure 9 Temporal evolution of Doppler velocity obtained on 2014 February 19 from Mg II k 2796 Å line intensity for two signals with height difference. The blue and red dashed lines refer to the first signal (near the limb) and the second signal (with distance of Y=5 arcsec), respectively.

By collecting this information for some time, a while, a set of time signals is obtained. It can be said that signals are a set of physical quantities that change according to an independent parameter or variable. If the variable is time, the signal is a temporal signal, and if it is location, it is called a spatial signal. These signals contain information about their sources and by processing the signals, the behavior of the sources can be analyzed.

4. Conclusion and Discussion

In this study, using spectral images obtained from the IRIS Telescope by spectral analysis, we were able to detect Doppler shift fluctuations of EEs. By analyzing the spectral profiles for two altitudes across the slit, we determined the amplitude of the Doppler velocity for two data. Doppler velocity in the first data for the two altitudes was obtained about -50 km/s to 50 km/s. De pontieu et al. (2014) studied prevalence of small-scale twist in the solar chromosphere and transition region and found rapidly evolving twisting motions are apparent as short-lived, bright features in the blue and red wings around ±50 km/s of the chromospheric Mg II h 2803Å spectral line. We calculated the phase velocity of the oscillations using a technique based on cross-correlation. The phase velocity is obtained as about 220 km/s. Because the spicules are almost in the vertical direction on the slit, the resulting velocities due to fluctuations along the line of sight can be considered the transverse velocities of the EEs. component in It should be noted that in these observations

most of the Doppler shifts related to the events shown in this research are in the transverse direction to the local surface normal. The contribution of kink modes, which are parallel to the plane of sky, cannot be detected by observer, because such Doppler velocities have no along the line of sight. Photospheric convective motions are often the source of wave excitation in magnetic tubes (Zaqarashvili *et al.* 2003, Zaqarashvili *et al.* 2007). Therefore, the propagation of waves in the chromosphere can be traced through the dynamics of the EEs. In De Pontieu *et al.* (2004) authors indicated that the high heat and density of materials inside the EEs, and, most importantly, their tilt, increase the period of wave propagation inside them, so that even waves with 5-minute periods can propagate. Magnetic tubes conduct three types of waves: kink waves, sausage waves, and rotating Alfven waves. Some of these waves can cause Doppler displacement observations. Rotating Alfven waves in thin tubes cause periodic non-thermal flattening of spectral lines but do not cause Doppler displacement fluctuations (Zaqarashvili *et al.* 2003). Sausage waves cause fluctuations in the intensity of the lines due to density changes, and if the axis of the tube is at an angle to the vertical line, the longitudinal velocity field of the sausage waves can cause Doppler displacement changes. However, the main contribution to Doppler displacement fluctuations is due to kink waves, which fluctuate transversely perpendicular to the axis of the tube (Zaqarashvili *et al.* 2007). In Pasachov *et al.* (2009) the unsigned line of sight velocities of the spicules were determined slightly fewer than 10 km/s. In De Pontieu *et al.* (2007) and Pereira *et al.* (2012) the velocities perpendicular to the main axis of the spicules were determined between 5 and 30 km/s. For example, in De Pontieu *et al.* (2012) two types of transverse motions in spicules are identified: 1) Swaying motions of 15 to 20 km/s and 2) Torsional motions in the range of 24 to 20 km/s. They reported that Alfven waves with amplitudes of 10 to 25 km/s with periods of 100 to 500 seconds could penetrate chromosphere. When plasma flows in opposite directions from the source, the Doppler Effect could be generated. In this case, strong enhancement in TR spectra is observed and has been known as bi-directional jets in which plasma moving along magnetic field lines (Curdt *et al.* 2011). Such Doppler velocities can be generated by any mechanisms that can produce bi-directional flows within the space of the pixel size. Explosive events are usually originated from magnetic reconnections (Hong *et al.* 2014), and the wing enhancement indicates bi- direction reconnection jets with speeds of 50 to 200 km/s. Rouppe van der Voort et.al (2015) analyzed short-lived asymmetries in chromospheric spectral lines base on IRIS and Swedish Solar Telescope (SST). They found clear signatures of RBEs and RREs in Mg II h & k with asymmetries in spectral profiles and spectral signatures for RBEs and RREs in C II 1335 and 1336 Å and Si IV 1394 and 1403 Å spectral lines, that was interpreted as disk counterpart of type II spicules in uperchromosphere.

In Tavabi and Koutchmy (2019) authors investigated properties of the spicules-material off-limb above the 2.2 Mm heights using IRIS observations. They suggested that numerous small-scale jet-like spicules show rapid twisting and swaying motions evidenced by the large distortion and dispersion of the line profiles, including impressive periodic Doppler shifts, with an average swaying speed of order ±35 km/s reaching a maximum value of 50 km/s in the polar coronal hole region. They also identified for the first time waves with a short period of order of 100 s and less and transverse amplitudes of order of ± 20 to 30 km/s with the definite signature of Alfven waves. In Tei *et al.* (2020), by analyzing the Mg II spectrum, the speed of the spicules along the field of view was obtained from -25 to 25 km/s so that the average asymptomatic speed of the spicules was from 2 to 10 km/s. According to the Doppler effect, the extended strong wings in the TR spectra indicate the existence of opposite-directional plasma flows in the source. Therefore, transition region EEs (TREEs) have also been known as "bi-directional jets". Chen et al. (2019) studied a statistic analysis at Si IV spectra for finding the connection between TREEs and network jets. They found several types of EEs: TREEs with double peaks or enhancements in both wings located at either the footpoints of network jets, or transient compact brightenings which most likely due to magnetic reconnection, TREEs with enhancements only at the blue wing located above network jets along their propagating directions which clearly result from the superposition of the high-speed network jets on the TR background, TTEEs showing enhancement only at the red wing of the line generally located around the footpoints of network jets, likely due to the superposition of reconnection downflows on the background emission, and TREEs not corresponded to network jets associated with small-scale transient bright points in the SJI 1330 °A images, which could be characterized as quiet-Sun UV bursts.

Bruceckner and Bartoe (1983), called as "Turbulent Events", the size varies from less than 1 arcsec, which is the resolution limit of instrument, to 4 arcsec. The line profiles of TEs show a strong, non-Gaussian enhancement of both the long-wavelength and short wavelength wings (C IV, $1x10^5$ K and also seen in C II $2x10^4$ and N v $2x10^5$ K). However, asymmetries in both directions have been observed velocities rang from +/-50 to +/-250 km/s. Hansteen et al. (2014) investigated a similar phenomenon and named as Unresolved Fine Structure (UFS), they were aligning the slit along the limb, IRIS also allows one to gather spectral data of the UFS. The spectrum shows large excursions as a function of position along the loop, implying large plasma velocities, towards the red as well as towards the blue. They found extreme line profiles at the upper loop foot point – the portion of the loop which meets the underlying atmosphere -

during the entire 200 s lifetime of the UFS loop, with red-ward excursions of 70-80 km/s. This is two to three times the speed of sound in a 80,000-100,000 K plasma. They observed the spectral properties of several UFS loops and find that such high velocities occur often, though not always. This indicates that the UFS loops are locations of episodic and violent heating.

About Alfvenic structure the asymmetric (with a tilt angle) profiles on the red and blue wing of the events could be explained by a rotational ejection. Tavabi et al. (2015) studied in details the position of the EEs, and showed the very rapid blue- and co-temporal redshifts, in the C II and Mg II k raster Dopplergrams in the velocity space, that described in the literature as Alfvénic waves propagation (Brueckner & Bartoe 1983; Martinez-Sykora et al. 2015, Sadeghi and Tavabi 2022). Rompolt (1974) interpreted all shapes of spectral features (lines) from the expected of rotating, expanding. He considers that the observed inclination to the direction of dispersion of some spectral features can be produced by rotation but not by expansion with the observational evidences.

De Ponteiu et al. (2012) showed that the tilted-streak morphology indicates relative redshift on one side of a spicule, blueshift on the other. This reversal in transverse motion is the signature of torsional spicule motion. In addition, the substantial offsets of the tilted streaks from the nominal line center can be understood as the upper position of swaying motion and a projection of field-aligned flow onto the line of sight. Tavabi t al. (2011) used the time slice Hinode Ca II H line with unprecedented spatial resolution, demonstrated that almost this spectrum tilt angle related to the rotational motion such as Alfvenic torsional behavior. In conclusion, according to the periodic red and blue enhancements in EEs, we suggested that the fluctuations in the EEs with one side enhancement indicate the swaying motions of spicules over their axes, and those EEs which observed on both wings indicate the rotational motions of spicules. The swaying and rotating motions are responsible to kink and twisted waves respectively.

Acknowledgements: We warmly acknowledge the work of our referee, who provided an extended detailed report and added many interesting suggestions and requests for greatly improving the paper. The authors gratefully acknowledge the use of data from the IRIS databases. IRIS is a NASA small explorer mission developed and operated by LMSAL with mission operations executed at NASA Ames Research center and major contributions to downlink communications funded by ESA and the Norwegian Space Centre.

REFERENCES

Bose, S., Henriques, V. M. J., Joshi, J., Rouppe van der Voort, L.: 2019, A&A, 631L, 5B

Bose, S., Rouppe van der Voort, L., Joshi, J., Henriques, V. M. J., Nóbrega-S., et al., 2021a, A&A, 654A, 51B

Bose, S., Joshi, J., Henriques, M. J., Rouppe van der Voort, L.: 2021b, A&A, 647A, 147B

Brueckner, G.E., and Bartoe, J.-D.F.: 1983, *ApJ*, **272**, 329

Chae, J., Wang, H., Lee, C.-Y., Goode, P.R., and Schuhle, U.: 1998, *ApJ*, **504**, L123

Chen, Y. J., Tian, H., Huang, Z., Peter, H., and Samanta, T.: 2019, *ApJ*, **873**, 79.

Curdt, W. and Tian, H.: 2011, *Astron. Astroph*, **532**, L9.

Curdt, W., Tian, H., and Kamio, S.: 2012, *SoPh*, **280**, 417

De Pontieu, B., McIntosh, S. W., Carlsson, M., Hansteen, V. H., Tarbell, T. D., Schrijver, C. J., et al.: 2007, *Science*, **318**, 1574

De Pontieu, B., McIntosh, S.,Hansteen, V. H., Carlsson, M., Schrijver, C. J., Tarbell, T. D., et al.: 2007a, PASJ, **59S**.655D

De Pontieu, B., Rouppe van der Voort, L., McIntosh, S. W., Pereira, T. M. D., Carlsson, M., Hansteen, V., et al.: 2014, *Science*, **346**,

De Pontieu B., Erd_elyi, R., James S. P.:2004, *Nature*, **430**, 536

De Pontieu, B., Carlsson, M., Rouppe van der Voort, L. H. M., Rutten, R. J., Hansteen, V. H., and Watanabe, H.: 2012, *ApJ*, **752**, L12

De Pontieu, B., Title, A. M., Lemen, J. R., Kushner, G. D., Akin, D. J., Allard, B., et al. 2014, *SoPh*, **289**, 2733

De Pontieu, B., McIntosh, S. W., Carlsson, M., Hansteen, V. H., Tarbell, T. D., Boerner, P., Martinez-Sykora, J., Schrijver, C. J., and Title, A. M. 2011, Science, **331,** 55

Dere, K.P., Bartoe, J.-D.F., and Brueckner, G.E.: 1984, *ApJ*, **281**, 870

Dere, K.P., Bartoe, J.-D.F., and Brueckner, G.E.: 1989**,** *SoPh*, **123**, 41.

Dere, K.P.: 1992, Solar Wind Seven Colloquium, 11

Doyle, J. G., Popescu, M. D.,and Taroyan, Y.:2006, *Astron. Astroph*, **446**, 327

Hansteen, V., De Pontieu, B., Carlsson, M., Lemen, j., Title, A., Boerner, P.: 2014, Science, 346E.315H

Hurlburt2, T.D. Tarbell2, J.P. Wuelser2, T.M.D. Pereira1, E.E. De Luca3, L. Golub3, S. McKillop3, Hong, J., Ding, M.D., Li, Y., Fang, C., and Cao, W.: 2014, *Astrophys*. J, **792**, 13

Innes, D. E., Inhester, B., Axford, W. I., Wilhelm, K. 1997, *Nature*, 386, 811

Kuridze, D., Henriques, V., Mathioudakis, M., Erdélyi, R., Zaqarashvili, T. V., Shelyag, S., Keys, P. H., Keenan, F. P.: 2015, ApJ, **802**, 26K

Langangen, _., De Pontieu, B., Carlsson, M., Hansteen, V. H., Cauzzi, G., and Reardon, K.: 2008, *ApJ*, **679**, L167

Leenaarts, J., Pereira, T. M. D., Carlsson, M., Uitenbroek, H., De Pontieu, B.: 2013a, *ApJ*, **778**, 143;

Leenaarts, J., Pereira, T. M. D., Carlsson, M., Uitenbroek, H., De Pontieu, B.: 2013b, **772**, 90L

Martinez-Sykora, J., Rouppe van der Voor, L., Carlsson, M., De Pontieu, B., Pereira, T., Tiago, M. D., Boerner, P., Hurlburt, N., Kleint, L., Lemen, J., Tarbell, T., Title, A., Wuelser, J. P., Hansteen, V. H., Golub, L., Mckillop, S., Reeves, K. K., Saar, S., Testa, P., Tian, H., Jaeggli, S., Kankelborg, C.: 2015, The Astrophysical Journal**. 803**, 9

Ning, Z., Innes, D., and Solanki, S.: 2004, Astron. Astroph, **419**, 1141

Pereira, T. M. D., De Pontieu, B., and Carlsson, M.: 2012, *ApJ*, **759**,18

Pasacho_, J. M., Jacobson, W. A., and Sterling, A. C.: 2009, *SoPh*, **59**

Pereira, T. M. D., De Pontieu, B., Carlsson, M., Hansteen, V., Tarbell, T. D., Lemen, J., et al., 2014.: *ApJ*, **792**, L15

Peter, H., Tian, H., Curdt, W., Schmit, D., Innes, D., De Pontieu, B., Lemen, J., Title, A. et al.: 2015, *Science*, **346**, 1255726

Roberts, B.: 2004, MHD Waves in the Solar Atmosphere, *ESA SP*, 547

Rompolt, B, 1975, *SoPh*, 41, 329

Rouppe van der Vo ort, L., Leenaarts, J., de Pontieu, B., Carlsson, M., and Vissers, G.: 2009, *ApJ*, **705**

Sekse, D. H., Rouppe van der Voort, L., De Pontieu, B.: 2012, ApJ, **752**, 108S

Sekse, D. H., Rouppe van der Voort, L. ; De Pontieu, B. ; Scullion, E.: 2013, ApJ, **769**, 44S

Sadeghi, R., Tavabi, E.: 2022, MNRAS, arXiv:2203.00665

Tavabi, E., Koutchmy, S., Ajabshirzadeh, A.: 2011, New Astron. 16, 296

Tavabi, E., Koutchmy, S., and Golub, L.: 2015a, *SoPh*, **290**

Tavabi, E., Koutchmy, S., Ajabshirizadeh, A., Ahangarzadeh Maralani, A. R., and Zeighami, S.,: 2015b, *Astron. Astroph*, **573,** 7

Tavabi E., Ajabshirizadeh A., Ahangarzadeh Maralani A. R., and Zeighami S. 2015c, *J. Astrophys. Astron*, **41**, 18Z

Tavabi, E.: 2018, *MNRAS*, **476,** 868

Tavabi, E., and Koutchmy, S.: 2019, *ApJ*, **883**, 41T

Tei, A., Gun, S., Heinzel, P., Okamoto, T., Stepan, J., Jejcic, S., and Shibata, K.:2020, *ApJ*, **888**, 2T

Zaqarashvili, T. V.: 2003, *Astron. Astroph*, 399L

Zaqarashvili, T. V., Khutsishvili, E., V. Kukhianidze, V., and Ramishvili, G.: 2007b, *Astron. Astroph*, **474**, 627

Zeighami, S., Ahangarzadeh Maralani, A. R., Tavabi, E., and Ajabshirizadeh, A.:2016, *SoPh*., **291**, 847858.

Zeighami, S., Tavabi, E., and Amirkhanlou, E.: 2020, *JApA*, **36**, 307T.

Zhang, M., Xia, L.-D., Tian, H., and Chen, Y.: 2010, *Astron. Astroph*, **520**, A37.